Int. J. Electrochem. Sci., 10 **(2015)** 2220 - 2238

International Journal of
ELECTROCHEMICAL
SCIENCE
www.electrochemsci.org

Psidium Guajava Leaf Extract as Green Corrosion Inhibitor for Mild steel in Phosphoric Acid

S. Noyel Victoria[1], *Rohith Prasad*[1], *R. Manivannan*[2,*]

[1]Department of Chemical Engineering, National Institute of Technology-Karnataka, Surathkal, India – 575 025.
[2]Department of Chemical Engineering, National Institute of Technology-Raipur, Chhattisgarh, India – 492 010.
[*]E-mail: rmani.che@nitrr.ac.in

Received: 12 October 2014 / *Accepted:* 25 December 2014 / *Published:* 19 January 2015

The adsorption and corrosion inhibition property of the alcoholic Psidium guajava (guava) leaf extract on mild steel in 1M phosphoric acid medium was investigated by weight loss, potentiodynamic polarization and electrochemical impedance spectroscopy techniques. The studies showed that the inhibition efficiency increases with inhibitor concentration upto 800 ppm and decreases slightly at 1200 ppm. The adsorption obeys both the Langmuir and the Temkin adsorption isotherm equations. The kinetic and thermodynamic parameters were calculated and discussed. The adsorption was found to follow a comprehensive type adsorption dominated by chemisorption. Potentiodynamic polarization studies showed that the inhibitor acted as a mixed-type inhibitor.

Keywords: Mild steel, corrosion, adsorption, EIS, Tafel.

1. INTRODUCTION

Mild steel is one of the industrially important metals. Use of corrosive chemicals in industries is unavoidable, which could lead to the dissolution of the metal. To protect the metal surface from the aggressive environment, various techniques such as corrosion protection coating, cathodic protection, anodic protection and inhibitors are available at the industrial level. Among the available measures for corrosion prevention, use of corrosion inhibitors is preferred widely since the quantity of inhibitor needed for observing the fruitful result is usually less [1]. Various synthetic organic and inorganic chemicals have been studied as corrosion inhibitors for mild steel in different aqueous media [2]. Synthetic inhibitors being toxic in nature are less preferred, which has made the exploration of natural compounds which have a strong affinity towards the metal surface important [3]. This group of

compounds called as green corrosion inhibitors are organic compounds that prevent corrosion by adsorbing onto the metal surface. The polar functions of these molecules with S, O or N atoms, heterocyclic compounds and p electrons are believed to be responsible for corrosion inhibition capacity of green corrosion inhibitors [3]. Many synthetic chemicals which are benign to the environment have also been studied as an alternate to the toxic organic chemicals [4-20]. Various organic compounds, namely surfactants, bis-(2-benzothiazolyl)-disulfide, dye, some antibiotics and antihistamines, thiourea, caffeic acid, aminoacids, betanine, guanidine derivatives, barbiturates, phenyldimethylsulfoniumbromide, azole derivatives and heterocyclic acids have been reported as environmental friendly corrosion inhibitors for mild steel in various acid media [4-20]. Relatively few works of the aforesaid groups have studied the corrosion in phosphoric acid medium [16, 18-20].

The corrosion inhibitors of plant origin are highly preferred because they are readily available, inexpensive with an advantage of environmentally benign nature. There are many studies which report the use of leaves, bark, fruits and vegetables of different plants as green corrosion inhibitor for mild steel in various aggressive media [21-33]. Extracts from *Pisidiumguajava*, *Punicagranatum*, *Ginkobiloba*, *Tinosporacrispa*, *Ficuscarica*, *Uncariagambir*, *Phyllanthusamarus*, *Murrayakoenigii*, *Justiciagendarussa*, *Azadiractaindica*, *Hibiscus sabdariffa* and *Zenthoxylumalatum* have been studied as corrosion inhibitors for mild steel in various acidic media [21-33]. The corrosion inhibition property of *Pisidium guajava* leaf extract on mild steel in 1 M HCl was characterized electrochemically by Anupama and Abraham [21]. Their results showed that the corrosion current (I_{corr})dropped significantly with increasing inhibitor concentration and the adsorption was found to follow Frumkin isotherm [21]. Phosphoric acid is widely used in fertilizer plants. Phosphoric acid manufactured by wet process is highly corrosive depending upon the impurities concentration [33]. Very few works report corrosion inhibitors for mild steel in phosphoric acid medium [2, 16, 18-20, 28, 33,34]. Phenacyldimethylsulfonium bromide and it's derivatives were studied for their corrosion inhibition property on mild steel in 2N phosphoric acid media. The highest efficiency obtained was 84.82% at a concentration of 0.005 M for the inhibitor [18]. There are some works which report the use of organic compounds such as quaternary N-heterocyclic compounds, 2-mercaptobenzimidazole, triazoles for mild steel corrosion prevention in phosphoric acid medium [19, 20]. However, much less work reports the use of green corrosion inhibitor for mild steel in phosphoric acid medium [2, 33]. Apricot juice has been reported to have good corrosion inhibition properties on mild steel in 1M H_3PO_4 [28]. *Zenthoxylum alatum* has been tested for its corrosion inhibition efficiency in various concentrations of phosphoric acid [33]. The use of sulphur containing amino acids in combination with Cl^-, F^- and Fe^{3+} ions was found to be effective against corrosion of mild steel in phosphoric acid medium [34].

A detailed investigation was conducted on the use of guava leaf extract as green corrosion inhibitor for mild steel in 1 M phosphoric acid. The corrosion inhibition properties were characterized by weight loss measurements, potentiodynamic polarization and electrochemical impedance spectroscopy measurements (EIS) studies. The surface of the samples was analysed using scanning electron microscopy (SEM) to study the effect of the inhibitor on mild steel surface. The surface of the mild steel treated the guava leaf extract was analysed by Fourier transform infrared spectroscopy (FTIR) to characterize the interaction between metal and plant extract.

2. EXPERIMENTAL

2.1. Preparation of plant extract

Dried guava leaves (100 g) were powdered and soaked in 500 mL methanol for 24 h. The mixture was then filtered and the filtrate was refluxed for 5 h at 50°C. The resulting liquid was concentrated using the vacuum evaporation setup and was used for the studies. The amount of solid in the sample was measured by evaporating a known volume of the extract to remove the methanol completely and weighing the residue.

2.2. Weight loss studies

Mild steel specimen with 0.2 wt% carbon content was used for the study. The weight loss studies were conducted by immersion of pre weighed mild steel coupons of 10 mm dia and 5 mm thick in the phosphoric acid solution. The weight loss studies were conducted at various concentrations of inhibitor and at various temperatures. Before the weight loss experiments, the mild steel coins were polished with 200, 400, 600, 800, 1000 and 2000 grades of SiC sand paper, washed with acetone and double distilled water. The washed coins were dried and weighed before immersion into the test sample. The effect of inhibitor concentration was studied by immersion of the coins for 60 min and also at 15 min at different inhibitor concentrations. The effect of temperature was studied with and without 800 ppm inhibitor with an immersion time of 15 min. The sample which was kept immersed in the test solution was taken out, washed and weighed upon drying. Corrosion rate in mg cm^{-2} s^{-1} was calculated from the weight loss of the specimen (mg), area (cm^2) and immersion time (s).

2.3. Electrochemical experiments

The electrochemical experiments were performed using Parstat 2263 potentiostat (Princeton applied research, USA). A three electrode cell was used for the measurements. The electrochemical experiments were conducted using a mild steel working electrode. The working electrode was fabricated from a mild steel rod of 5 mm dia and 15 mm length, which was sealed into a Teflon tube which had 7 mm hole. Silver-silver chloride electrode (Ag/AgCl) was used as reference and platinum gauze was used as the counter electrode. Millipore water was used for electrolyte preparation. Prior to each experiment, the working electrode was polished with various grades of sand paper washed and again polished with various grades of alumina powder. A stabilization period of one hour was allowed for potentiodynamic polarization and EIS experiments. Tafel runs were conducted in the potential range from -250 mV to +250 mV relative to the corrosion potential. A scan rate of 1 mVs^{-1} was used for the Tafel run. The Tafel extrapolation method was used in the calculation of corrosion current densities and other Tafel fit parameters. The EIS runs were conducted from 100 kHz to 0.1 Hz and a potential amplitude value of 10 mV rms was used. The impedance measurements were conducted at open circuit potential (OCP). The electrochemical experiments were conducted at room temperature and at various concentrations of phosphoric acid and extract.

2.4. Surface analysis

The surface analysis of the steel coupons was conducted by immersion of the cleaned sample in 1 M phosphoric acid solution with and without 800 ppm inhibitor for 6 h and washing and drying the coin. The coupons thus prepared were used for surface analysis. Surface analysis of coins was studied using scanning electron microscope.

2.5. FTIR analysis

The mild steel coin was immersed in 1 M phosphoric acid with 800 ppm extract for 6 h. The sample was taken out after 6 h, dried and the film formed on the surface was gently removed and used for FTIR analysis.

3. RESULTS AND DISCUSSION

3.1. Weight loss experiments

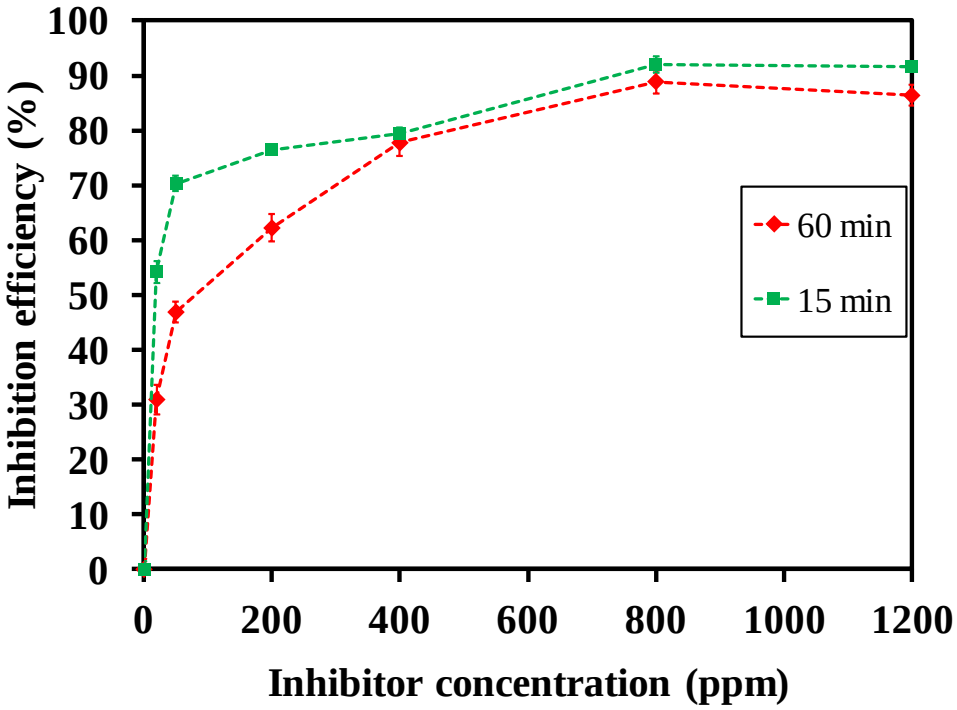

Figure 1. Effect of inhibitor concentration on the inhibition efficiency for mild steel in 1 M phosphoric acid solution. (The line in the Fig. is to guide the eye; it does not represent any data fit)

The inhibition efficiency for the mild steel coupons immersed in 1 M phosphoric acid solution with different inhibitor concentrations are shown in Figure 1. The inhibition efficiencies for 15 min

and 60 min immersion time are shown in Figure 1. The inhibition efficiency was calculated using the equation 1 [3].

$$\text{Inhibition efficiency (\%)} = \frac{W_0 - W_i}{W_0} \text{ x } 100 \qquad (1)$$

where, W_0 is the weight loss of the coupons in the absence of inhibitor, W_i is the weight loss of the coupons at a particular inhibitor concentration. It can be seen from Figure 1 that for 60 min immersion time, the inhibition efficiency increases with inhibitor concentration from 30% at 20 ppm to 89% at 800 ppm. The inhibition efficiency drops slightly to 87% for 1200 ppm extract. The increased inhibition efficiency with inhibitor concentration is believed to be due to the adsorption of inhibitor molecules on the metal /solution interface which increases with increased inhibitor concentration [21]. A slight drop in the inhibition efficiency at 1200 ppm inhibitor concentration may be due to the desorption of the inhibitor molecules back into the bulk on approaching the critical concentration. The desorption weakens the metal-inhibitor interaction resulting in a drop in inhibition efficiency [30, 35]. It can also be gathered from Figure 1 that at lower inhibitor concentrations, the inhibition efficiency drops with increased immersion time, whereas at higher concentrations the difference in the inhibition efficiencies with immersion time is not significant. The same trend has been observed for mild steel in HCl in the presence of cefazolin inhibitor [35].

3.2. Effect of temperature

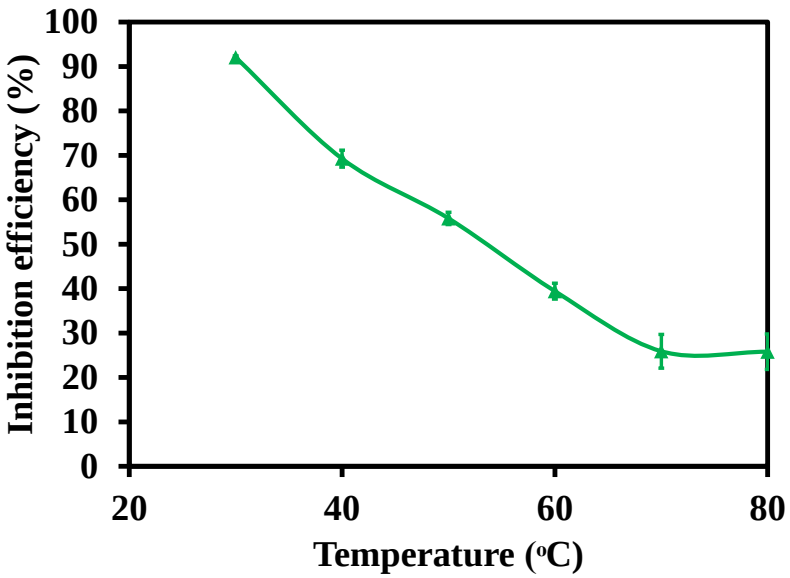

Figure 2. Inhibition efficiency at various temperatures for mild steel in 1 M phosphoric acid solution and 800 ppm inhibitor. (The line in the Fig. is to guide the eye; it does not represent any data fit)

The effect of temperature on the corrosion rate (*CR*) was studied for mild steel in 1 M phosphoric acid in the presence and absence of inhibitor. The temperature range studied were 30°C–80

°C. The inhibitor concentration taken in the studies was 800 ppm. The inhibition efficiencies at various temperatures in the presence of 800 ppm extract is shown in Figure 2.

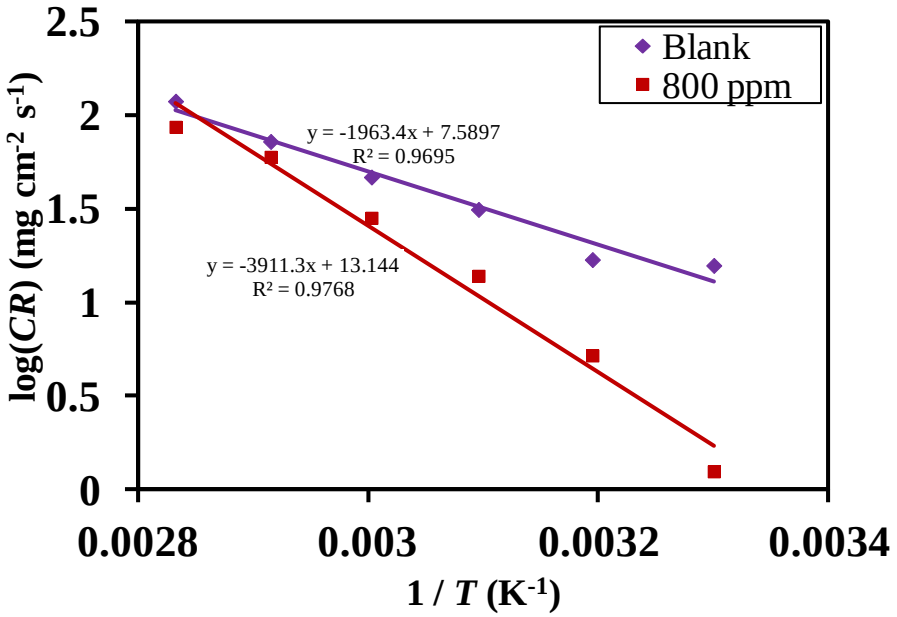

Figure 3. Arrhenius plots for mild steel in 1 M phosphoric acid solution with and without 800 ppm inhibitor.

The dissolution of mild steel in acidic medium increases with increase in temperature due to decrease in hydrogen evolution over potential [26]. This shows that the guava leaf extract is effective in minimizing the corrosion at higher temperatures to some extent. The inhibition efficiency of the extract drops with increasing temperature. The inhibition efficiency at 30°C was 92%, which falls to 27% at 80°C. The decrease in the inhibition efficiency could be due to increased dissolution of mild steel with increasing temperatures and desorption of the adsorbed inhibitor molecules from the metal surface [27]. The activation energy (E_a) for the system in the presence and the absence of inhibitor was calculated using the Arrhenius equation. The log (*CR*) obtained from the weight loss measurements was a linear function of temperature [27].

$$\log(CR) = -\frac{E_a}{2.303RT} + A \qquad (2)$$

where E_a is the apparent effective activation energy, R is the gas constant, A is the Arrhenius pre-exponential factor and T is the temperature. Figure 3 shows the Arrhenius plots for the mild steel in 1 M phosphoric acid with and without 800 ppm inhibitor. The E_a for the system in the absence of inhibitor was 37 kJ mol^{-1} whereas with 800 ppm inhibitor it was calculated to be 75 kJ mol^{-1}. The increase in E_a with the addition of inhibitors may be due to the increased energy barrier of the corrosion reaction [26]. When the inhibition efficiency drops with increasing temperature and the E_a in the presence of inhibitor is higher than the E_a in the absence of inhibitor, then the adsorptive film formed on the surface of the metal is believed to be due to physical adsorption [32]. A drop in inhibition efficiency can also be explained by increased dissolution of metal at higher temperature and weakening of the physisorbed inhibitor layer at higher temperatures in the presence of inhibitor [9].

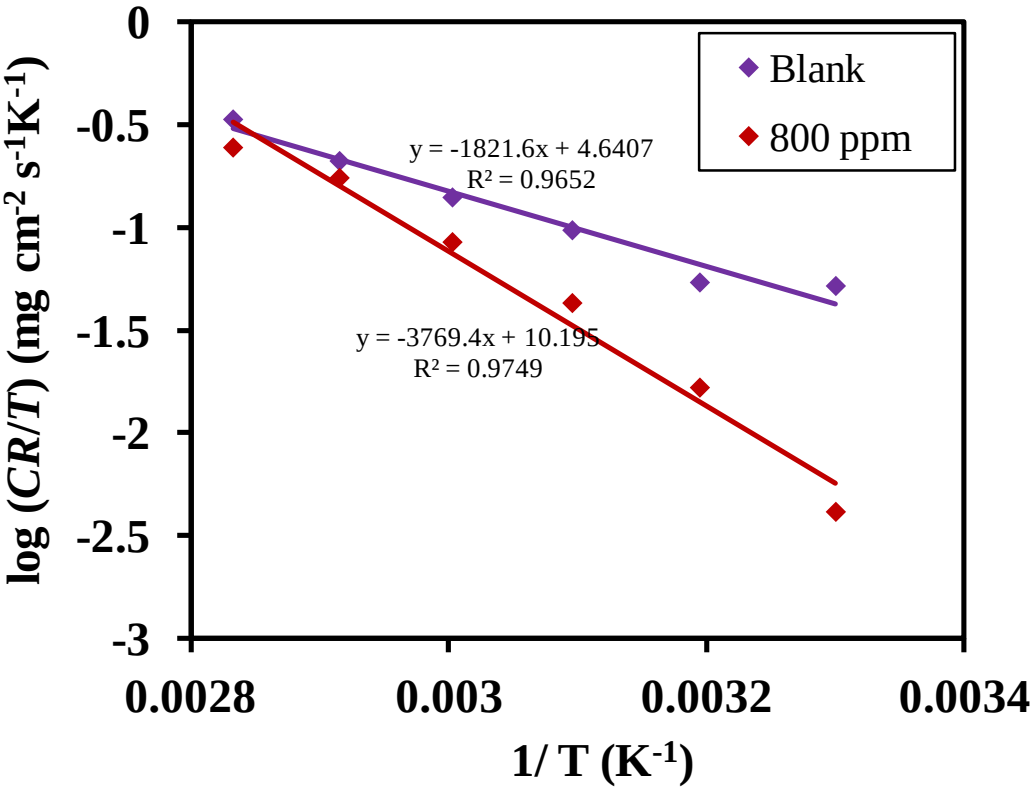

Figure 4. Plots of log (*CR/T*) vs. 1/*T* for mild steel in 1 M phosphoric acid with and without 800 ppm inhibitor.

However, literatures report adsorption processes with E_a less than 40 kJ mol^{-1} follow physical adsorption and those above 80 kJ mol^{-1} are typical to chemisorption. With the preceding relations it can be concluded that the guava leaf extract with an activation energy 75 kJ mol^{-1} follows comprehensive adsorption, which is a combination of both physical and chemical adsorption [33-35]. On the other hand, E_a is not a reliable parameter for characterizing the nature of adsorption because of the competitive adsorption with water molecules, the removal of which needs some activation energy [36]. To investigate the system thermodynamics further the enthalpy of activation (ΔH_a) entropy of activation (ΔS_a) for the system were calculated using the transition state equation 3 from the results of the weight loss experiments at different temperatures with and without 800 ppm inhibitor [10, 11, 37].

$$\log\left(\frac{CR}{T}\right) = \log\left(\frac{R}{Nh}\right) + \frac{\Delta S_a}{2.303R} - \frac{\Delta H_a}{2.303RT} \quad (3)$$

In equation 3, R is the universal gas constant, N is the Avogadro's number and h is the Planck's constant. A plot of log (*CR/T*) versus 1/*T* is shown in Figure. 4. The plot is a straight line with slope -ΔH_a/2.303R and log(R/Nh)+(ΔS_a/2.303R) as the intercept. The values of ΔH_a and ΔS_a in the presence and absence of 800 ppm inhibitor are shown in the Table 1.

Table 1. Thermodynamic parameters for mild steel in 1 M phosphoric acid with and without 800 ppm inhibitor

	Inhibitor concentration mg L^{-1}	
Parameter	**0**	**800**
ΔH_a (kJ mol^{-1})	34	72
E_a (kJ mol^{-1})	37	75
ΔS_a (J $mol^{-1}K^{-1}$)	-108	-2

The ΔH_a increases with the addition of the extract. The values match well with the literature values for mild steel in acidic medium with and without the inhibitor [10, 27]. A positive value of ΔH_a shows that the dissolution process is endothermic and that the dissolution in the presence of inhibitor requires more energy resulting in increased inhibition efficiency at lower temperatures [10].

The ΔS_a is negative in both cases with ΔS_a value for the system without inhibitor being more negative. A negative ΔS_a is an indication that the corrosion process is controlled by activation complex [10]. A closer look at the ΔS_a values shows that the values move towards a positive direction in the presence of the extract. Such a positive shift is due to the formation of the adsorbed layer on the metal surface, which is believed to increase the disorderliness of the system. The inhibitor layer hinders the liberation of hydrogen ions at the metal surface, causing increased disorderliness resulting in increased entropy of the system [10, 38].

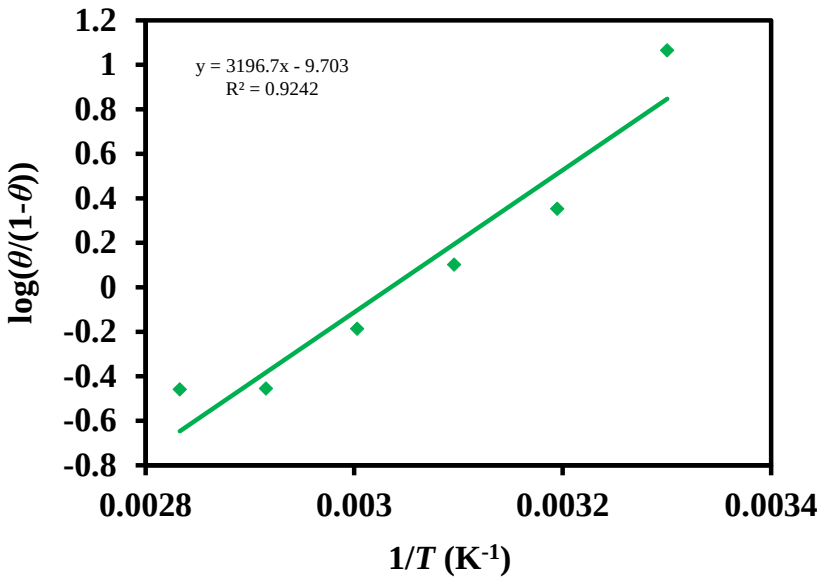

Figure 5. Plots of log (θ/(1-θ)) vs. 1/T for mild steel in 1 M phosphoric acid with 800 ppm inhibitor.

The heat of adsorption Q_{ads} can be considered equal to the enthalpy of adsorption (ΔH_{ads}) at constant pressure conditions [39]. The value of Q_{ads} for the system at a constant inhibitor concentration was calculated using equation 4 [39].

$$\log\left(\frac{\theta}{1-\theta}\right) = \log A + \log C - \frac{Q_{ads}}{2.303RT} \quad (4)$$

where θ is the surface coverage, A is a constant and C is the concentration of the inhibitor. Using the surface coverage values for the system with 800 ppm extract in the temperature range from 30°C to 80°C a plot of $\log(\theta/(1-\theta))$ vs. $1/T$ is constructed, which is shown in Figure. 5.

The slope of the straight line is $-\Delta H_{ads}/2.303R$. The value of ΔH_{ads} was calculated to be -61.2 kJ mol^{-1}. A negative value of ΔH_{ads} shows that the adsorption of the inhibitor molecule on mild steel surface is exothermic and a negative ΔH_{ads} value can signify either a physisorption or chemisorption process. An absolute ΔH_{ads} value of 41.86 kJ mol^{-1} or lower is considered as physisorption and that is higher than 100 kJ mol^{-1} is chemisorption [35]. Since the present system yields a ΔH_{ads} of -61.2 kJ mol^{-1}, it can be considered an intermediate between chemical and physical adsorption, which is comprehensive adsorption [35-40].

3.3. Potentiodynamic polarization studies

The results of potentiodynamic polarization experiments with mild steel as the working electrode in 1 M phosphoric acid at different concentrations of the inhibitor are shown in Figure. 6. The corrosion current (I_{corr}) values calculated by linear extrapolation of the Tafel plots are shown in the Table 2.

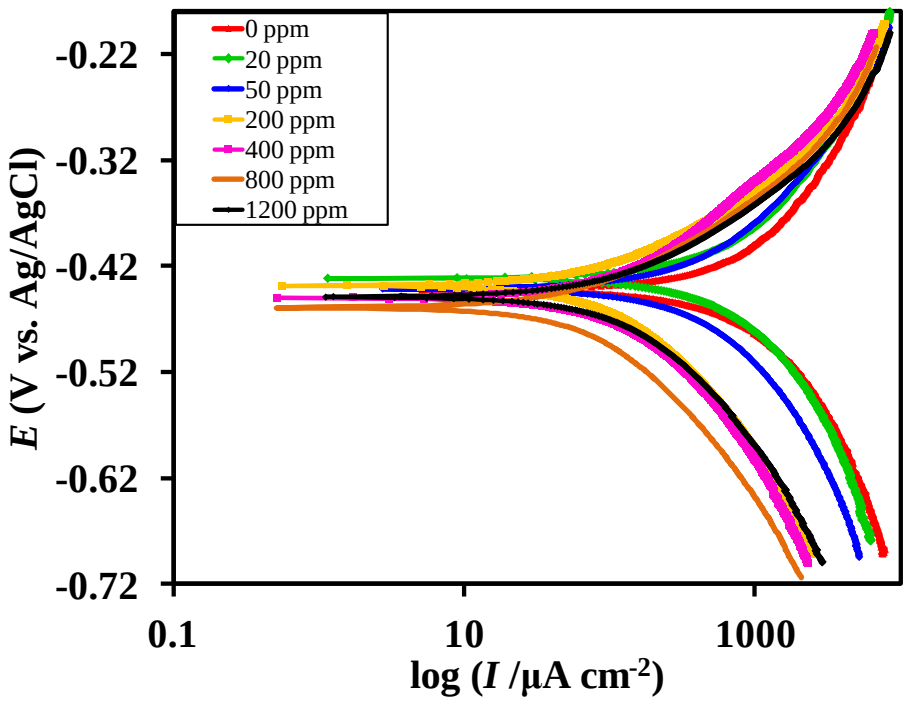

Figure 6. Potentiodynamic polarization plots for mild steel in 1 M phosphoric acid at various inhibitor concentrations. The scan rate used was 1 mV s^{-1}.

Table 2. Tafel parameters and inhibition efficiency for mild steel in 1 M phosphoric acid at various inhibitor concentrations

Concentration (mg L^{-1})	**E_{corr} (mV vs. Ag/ AgCl)**	**I_{corr} (μA cm^{-2})**	**β_c (mV dec^{-1})**	**β_a (mV dec^{-1})**	**Inhibition Efficiency %**
0	-427	975	-256	204	0
20	-431	929	-260	229	5
50	-437	651	-255	192	33
200	-450	206	-205	131	79
400	-439	182	-214	127	81
800	-459	107	-178	104	89
1200	-456	252	-215	137	74

The inhibition efficiency was calculated from the I_{corr} values using equation 5 [27]

$$\text{Inhibition efficiency (\%)} = \frac{I^0_{Corr} - I^i_{Corr}}{I^0_{Corr}} \text{ x } 100 \quad (5)$$

In the above equation I^0_{corr} represents the corrosion current in the absence of inhibitor and I^i_{corr} is the corrosion current at any particular inhibitor concentration.

It can be seen from Figure 6 that the inhibitor addition reduces both cathodic hydrogen evolution and anodic metal dissolution reactions [39, 41, 42]. The I_{corr} values decrease significantly with increase in inhibitor concentration up to 800 ppm and increases slightly at 1200 ppm. The corrosion potential values (E_{corr}) show a shift towards more negative potential with increase in inhibitor concentration up to 800 ppm. The E_{corr} value changes slightly to the positive side for 1200 ppm extract concentration. A negative shift in the E_{corr} values with the addition of an inhibitor is characteristic of mixed type inhibitors.[41, 42] Moreover, literatures also suggest that if the maximum displacement in the E_{corr} is greater than 85 mV, then the inhibitor is cathodic or anodic and if it is less than 85 mV it is categorized as a mixed type inhibitor [24]. The maximum displacement in E_{corr} was calculated as 28 mV vs. Ag/AgCl which also shows that the extract acts as a mixed type inhibitor. The weight loss experiments also show a slight drop in the inhibition efficiency when the inhibitor concentration was increased from 800 ppm to 1200 ppm. A similar trend was observed when the *Zenthoxylum alatum* plant extract was used as inhibitor for mild steel in 20% phosphoric acid. A drop in inhibition efficiency and an increase in I_{corr} value were observed when the concentration was increased from 2400 ppm to 3200 ppm [33]. A drop in the inhibition efficiency at higher inhibitor concentrations could be due to the desorption of molecules form the metal surface [36, 41, 42]. It is observed from Figure.6 that the cathodic current-potential curves at different inhibitor concentrations are parallel to each other. This shows that the addition of inhibitor does not change the hydrogen evolution mechanism [36, 41, 42]. The reduction of H^+ ions at the mild steel surface takes place by charge transfer mechanism [36]. It can also be observed that the metal dissolution rate is lower in the presence of inhibitor at low anodic over potentials, it increases considerably at higher anodic over potentials. It can be explained that the inhibitor molecules form a film on the metal surface which

provides good corrosion protection at lower anodic over potentials. However, at higher anodic over potentials it loses its inhibitory effect [39].

3.4. Electrochemical impedance spectroscopy experiments (EIS)

The impedance data from a system can be tested for their stability, causality and linearity using Kramers Kronig Transformation (KKT) [43]. The most useful forms of KKT are as follows[44]

$$Z''(\omega) = \frac{2\omega}{\pi}\int_0^{\infty}\frac{Z'(x)-Z'(\omega)}{x^2-\omega^2}\mathrm{dx} \quad (6)$$

$$Z'(\omega) = Z'(\infty) + \frac{2}{\pi}\int_0^{\infty}\frac{xZ''(x)-\omega Z''(\omega)}{x^2-\omega^2}\mathrm{dx} \quad (7)$$

where Z' and Z'' are the real and imaginary impedance values, respectively. The ω is the angular frequency calculated using the relation $\omega = 2\pi f$, where f is the frequency in Hz. $Z(\omega)$ is the impedance expressed as a function of ω. The value of integrals in 6 and 7 is calculated using the $Z(\omega)$ based on experimental data recorded in a finite frequency range (ω_{min}, ω_{max}). It is interpolated to assure sufficient integration accuracy with small integration steps dx and extrapolated to $\omega \rightarrow 0$ and to $\omega \rightarrow \infty$ [44]. Figure 7 shows the KKT validation plots for the Z_{re} and Z_{im} values. It can be seen from the plots that the experimental and the calculated values match well. Figure 8 shows the Nyquist plots for mild steel in 1 M phosphoric acid medium at various inhibitor concentrations. The Nyquist plot shows a depressed semicircle for all the inhibitor concentrations.

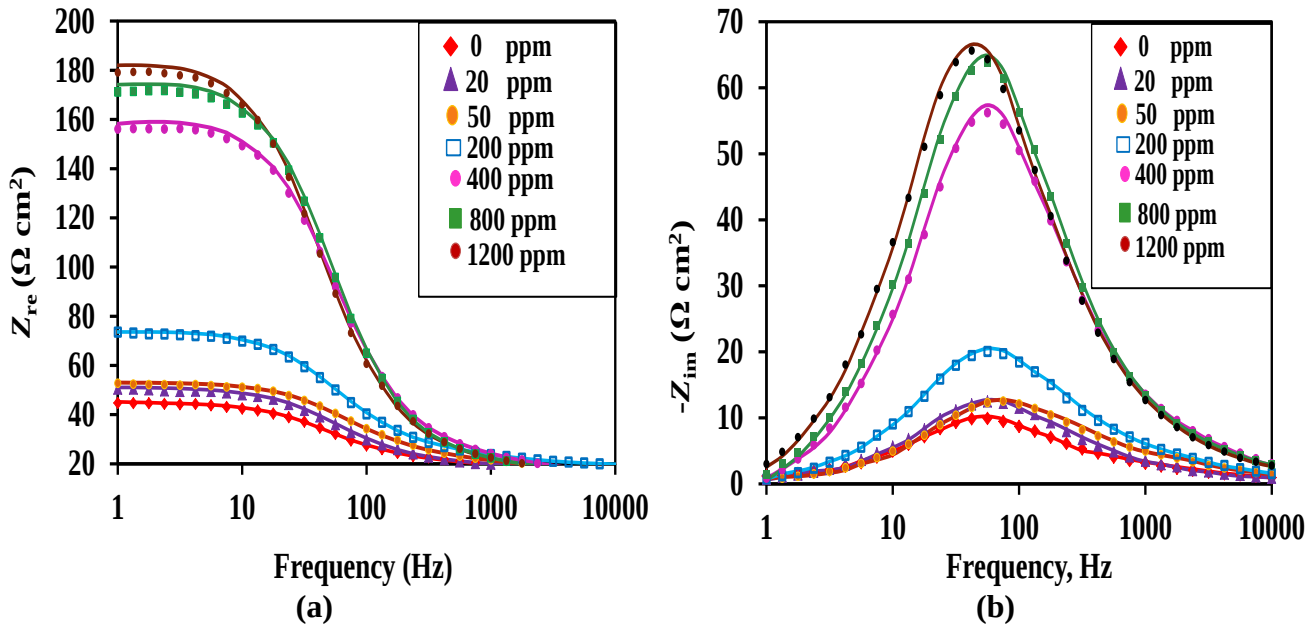

Figure 7. KKT fits for the EIS data for mild steel in 1 M phosphoric acid at various inhibitor concentrations. The solid lines represent the KKT fit. **(a)** KKT fits showing Z_{re} vs. frequency **(b)**KKT fits showing -Z_{im} vs. frequency.

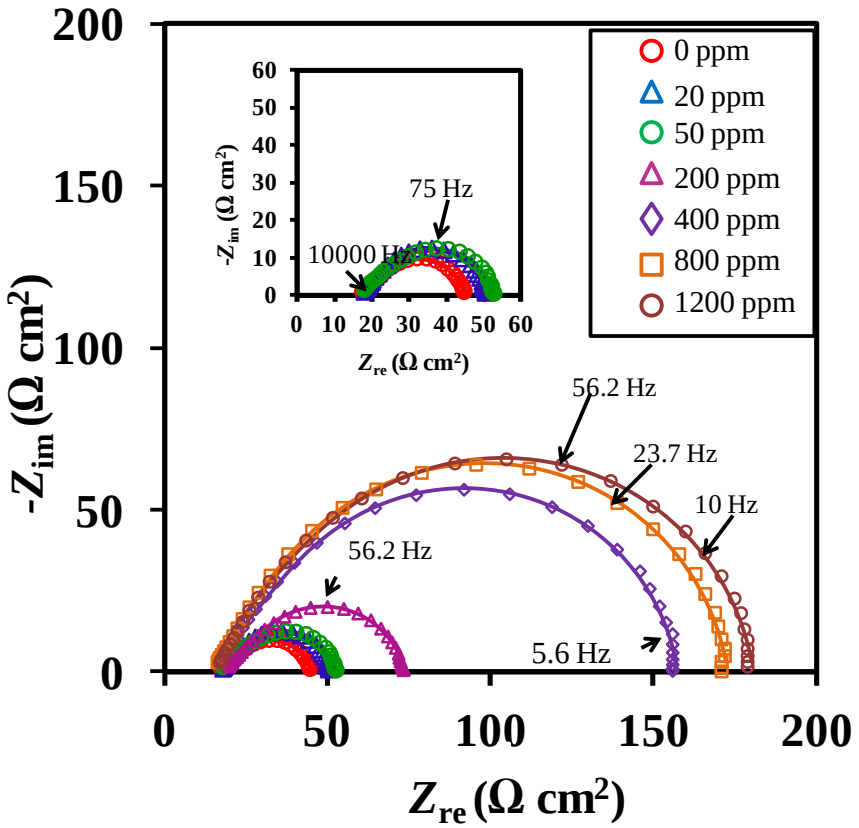

Figure 8. Nyquist plots for mild steel in 1 M phosphoric acid at various inhibitor concentrations at OCP. Inset figure shows the Nyquist plots for inhibitor concentrations 0,20 and 50 ppm (Line represents the EEC fit).

The high frequency loops with depressed semi-circular appearance are often referred to as frequency dispersion due to surface inhomogeneity or the roughness of the surface [26, 35]. Moreover, the impedance patterns show the formation of an arc in the low frequency end, which is attributed to the relaxation process obtained by the adsorbed species or re-dissolution of the passivated surface at lower frequencies [26, 35]. The Nyquist plots were modelled with an electrical equivalent circuit (EEC) which is made up of three resistances and two constant phase elements (CPE) which were used for modelling many dissolution systems [8, 43, 45]. The presence of depressed semicircle is attributed to the non-uniformity and surface roughness of the metal electrode,[35] hence CPE were used instead of ideal capacitors. A CPE can be considered a parallel combination of a pure capacitor and a resistor being inversely proportional to the angular frequency [26]. When the impedance pattern presents a depressed semicircle, the metal-solution interface is considered to act as a capacitor with irregular surface, which is a condition explained by CPE [26]. A CPE is defined by the mathematical expression given by equation 8 [26].

$$Z_{\mathrm{CPE}} = \frac{1}{Y_0 (j\omega)^n} \qquad (8)$$

Z_{CPE} in equation is the impedance of CPE, $\boldsymbol{Y_0}$ is the proportionality constant, ω is the angular frequency and n is the surface roughness parameter [26, 43, 44].

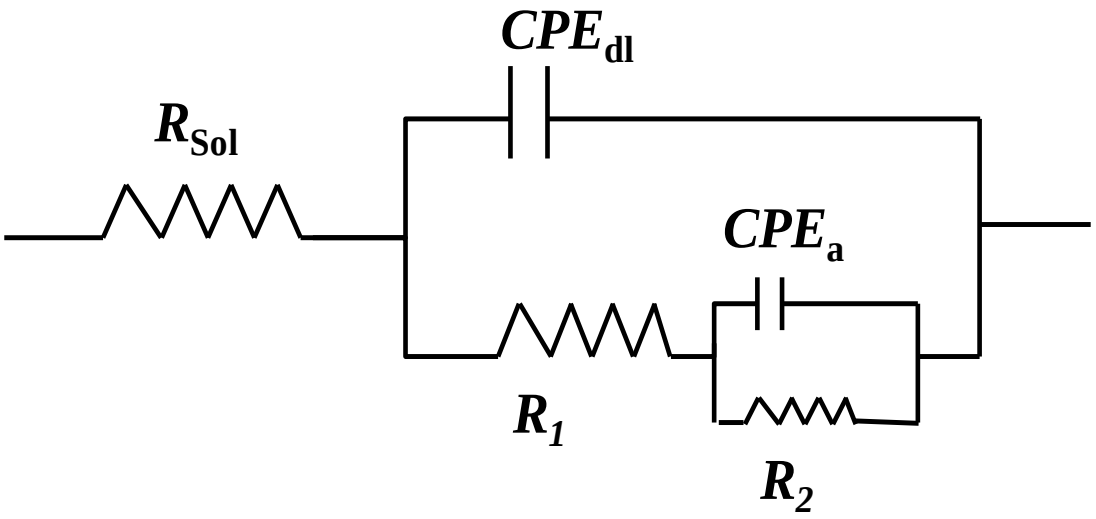

Figure 9. Electrical equivalent circuit (EEC) for 1 M phosphoric acid at various inhibitor concentrations

The corresponding circuit is shown in Figure 9. In the circuit R_{sol} represents the solution resistance of the system, R_1 is the charge transfer resistance for the corrosion reaction and the double layer resistance, CPE_{dl} is the capacitance of the electrical double layer at the metal-solution interface, R_2 and CPE_a represent the pseudo resistance and pseudo capacitance of the adsorbed layer [8, 43, 45, 46]. To describe the formation of a small arc at the lower frequency end, a combination of negative resistance and CPE is used. This combination is widely used to represent the arcs with inductive behavior as it is hard to explain a physical viewpoint to use a high inductance [26]. The double layer capacitance (C_{dl}) was derived from the CPE parameters using the equation 9 [46].

$$C_{dl} = (Y_d R_1^{1-n_d})^{1/n_d} \quad (9)$$

The relaxation time constant (τ_d) of charge transfer process was calculated using equation 10 [46]

$$\tau_d = C_{dl} R_1 \quad (10)$$

Similarly the relaxation time constant (τ_a) for the adsorption process was calculated using equation 11.

$$\tau_a = C_a R_2 \quad (11)$$

The polarization resistance (R_p) for the system was obtained by the summation of R_1 and R_2 [8, 41-43, 46]. The inhibition efficiency was calculated from the corrosion resistance (R_p) values using the equation 12 [46].

$$E(\%) = \frac{R_p^i - R_p^0}{R_p^i} \text{ x } 100 \quad (12)$$

R_p^i is the polarization resistance at any particular inhibitor concentration and R_p^0 is the polarization resistance in the absence of inhibitor [42,44]. The relaxation times along with other circuit parameters and the inhibition efficiency are given in Table 3.

Table 3. EEC fit parameters with relaxation time constants

Con. (mg L^{-1})	R_{sol} (Ω cm^2)	Y_d (10^5 Ω^{-1} $s^n cm^{-2}$)	n_d	R_1 (Ω cm^2)	C_{dl} (µF cm^{-2})	τ_d (10^4s)	Y_a (10^5 Ω^{-1} $s^n cm^{-2}$)	n_a	R_a (Ω cm^2)	C_a (µFcm^{-2})	τ_a (10^3s)	*IE* %
0	17.1	2	0.77	9.7	31	3	10	0.93	18.3	62	1	-
20	17.7	7	0.87	6.8	22	1.5	10	0.84	26.3	32	1	15
50	17.4	6	0.85	10.7	16	1.8	10	0.86	24.81	38	1	21
200	19.4	4	0.86	13.2	12	1.5	9	0.86	41.2	36	1.4	49
400	17.1	1	0.93	36.2	11	2	3	0.89	104.2	15	1.5	80
800	16.4	2	0.93	41.3	12	4.8	2	0.88	115	9	1	82
1200	17.4	2	0.92	61.6	11	6.9	3	0.9	101.8	1.6	1.6	82

The C_{dl} values decrease with increase in inhibitor concentrations which could be due to the formation of a protective layer by inhibitor molecules [46]. The increase in the values of n_d with an increase in inhibitor concentration could be attributed to the decreased surface inhomogeneity due to adsorbed inhibitor molecules [46]. An increasing n_d value also signifies that the charge and discharge rates are decreased with increasing inhibitor concentration [46]. The values of n_a are lower when compared to n_d, which is explained by the energy dissipation within the adsorbed layer [46]. Similarly C_a values decrease with an increase in inhibitor concentration. This could be due to the adsorption of inhibitor molecules resulting in the reduction of the local dielectric constant [12,29,30]. The R_p is dominated by R_a. The inhibition efficiency increases with inhibitor concentration up to 800 ppm and saturates at 1200 ppm. Maximum efficiency of 82% was obtained from the EIS results.

3.5. Adsorption isotherm

The adsorption process of the inhibitor molecules on the metal surface is believed to occur with the desorption of water molecules at the metal surface, which is thus an exchange process [29, 40-42]. The weight loss measurements, potentiodynamic polarization and electrochemical impedance spectroscopy runs at different concentrations of inhibitor show increased inhibition efficiency with increase in the inhibitor concentration. This shows that the inhibitor adsorbs on the metal surface and that the surface coverage (θ) increases with increasing inhibitor concentration. The θ is calculated by dividing the inhibition efficiency by 100 [10]. The data were analysed using Langmuir and Temkin adsorption isotherm. The Langmuir adsorption isotherm can be shown by equation 13 [10].

$$\frac{C}{\theta} = \frac{1}{k_{ads}} + C \qquad (13)$$

where C is the concentration of the inhibitor, θ is the surface coverage and k_{ads} is the equilibrium constant for adsorption. The results of both weight loss and electrochemical runs were analysed for adsorption characterization. The Temkin isotherm can be expressed using the equation 14 [29].

$$\theta = \frac{-\ln k_{ads}}{2a} - \frac{\ln C}{2a} \qquad (14)$$

In the above equation k_{ads} is the adsorption equilibrium constant and a is the attractive parameter.

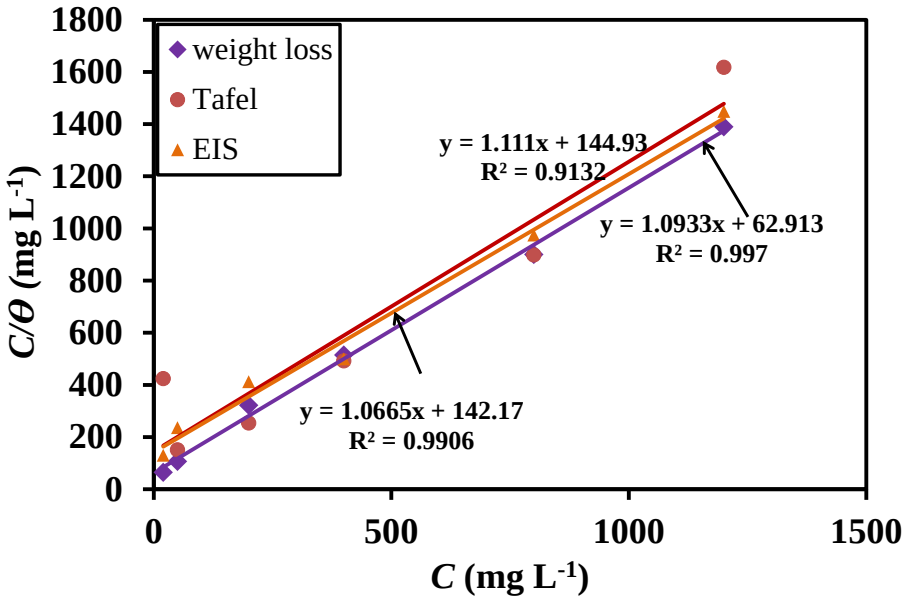

Figure 10. Langmuir adsorption isotherms for mild steel in 1 M phosphoric acid with and without 800 ppm inhibitor.

The Langmuir adsorption isotherm plots for weight loss, Tafel and EIS measurements are shown in Figure 10 and Figure 11 shows the results of the Temkin isotherm equation. The standard free energy of adsorption (ΔG°_{ads}) is calculated using the equation 14 [1].

$$\Delta G^{0}_{ads} = -RT\ln(k_{ads} \mathrm{x} \rho_{W}) \quad (15)$$

where R is universal gas constant, T is the absolute temperature in Kelvin, ρ_W is the density of water in g L^{-1}. The values of k_{ads} and ΔG°_{ads} for both Langmuir and Temkin isotherms calculated using the equations 13, 14 and 15 are listed in the Table 4.

Table 4. Langmuir adsorption isotherm parameters for mild steel in 1 M phosphoric acid with and without 800 ppm inhibitor

Parameter	Weight loss	Tafel	EIS
Langmuir			
k_{ads} (L g^{-1})	7.03	15.7	16.5
ΔG^{0}_{ads} (kJ mol^{-1})	-41	-39	-39
Temkin			
$\ln k_{ads}$ (L g^{-1})	6	4	4
ΔG^{0}_{ads} (kJ mol^{-1})	-33	-29	-28

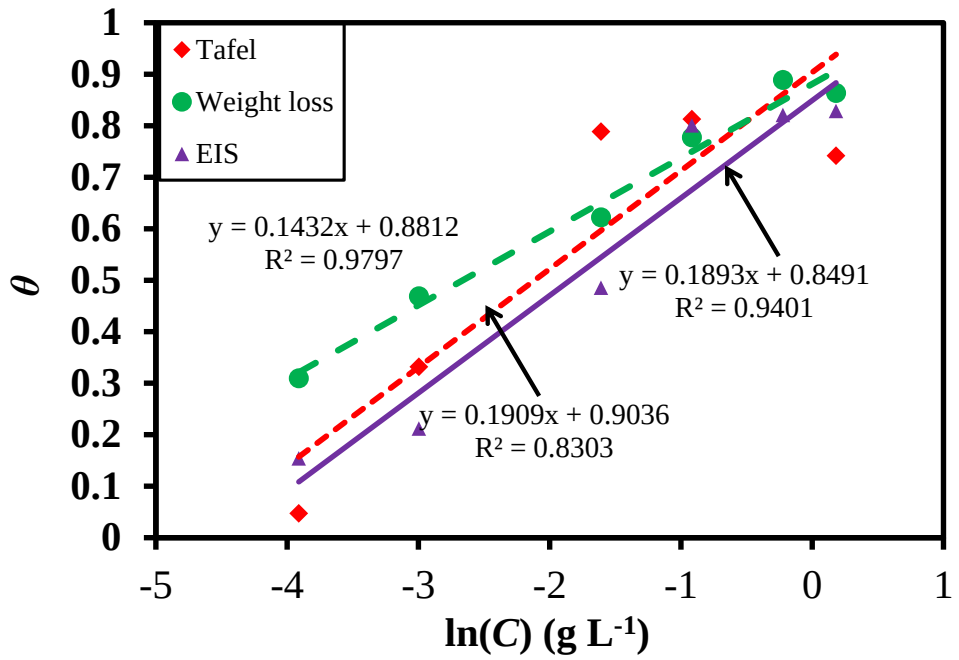

Figure 11. Temkin adsorption isotherms for mild steel in 1 M phosphoric acid with and without 800 ppm inhibitor.

The negative values of ΔG°_{ads} show that the adsorption process is spontaneous. The value of ΔG°_{ads} ranges between -39 kJ mol^{-1} and -41 kJ mol^{-1} for Langmuir adsorption isotherm. The Temkin isotherm yields ΔG°_{ads} values between -28 kJ mol^{-1} and -39 kJ mol^{-1}. A ΔG°_{ads} value of – 40 kJ mol^{-1} is considered the threshold value between chemical and physical adsorption processes [39-42]. Values up to -20 kJ mol^{-1} suggest physisorption and values more negative than – 40 kJ mol^{-1} are representative of chemisorption [39-42]. Thus, for the present system the ΔG°_{ads} values are in an intermediate range which suggests a comprehensive adsorption, a combination of both physical and chemical adsorption dominated by chemisorption.

3.6. Scanning electron microscopy

Figure 11 shows the SEM images of the mild steel specimens immersed in 1 M phosphoric acid solution in the presence and absence of 800 ppm inhibitor for 6 h. It is clearly seen that the surface of the sample which was immersed in phosphoric acid solution in the absence of inhibitor shows significant corrosion when compared to the sample kept in the presence of inhibitor.

3.7. FTIR analysis

The peaks from FTIR analysis of the sample obtained from mild steel coupons immersed in 1 M phosphoric acid solution containing 800 ppm extract are shown in Table 5.

Table 5. FTIR Peak locations for the sample from mild steel immersed in 1 M phosphoric acid with 800 ppm inhibitor

Frequency cm^{-1}	Band assignment
792	Iron oxide
1007	Iron phosphate complex
1250	-C-C stretch
1559.6	COO^- stretch
1620	Iron phosphate
2364.7	N-H stretching vibration
2981	-CH stretch
3100	N-H stretch
3674	OH stretching vibration
3838.1	OH stretching vibration

The bands at 1007 cm^{-1} and 1620 cm^{-1} show the presence of iron phosphate and the band at 792 cm^{-1} shows the presence of iron oxide [33]. The bands at 1250 cm^{-1}, 3100cm^{-1}, 2364.7 cm^{-1} and 2981 cm^{-1} could be attributed to the adsorption of plant extract molecules on mild steel surface [47].

3.8. Mechanism

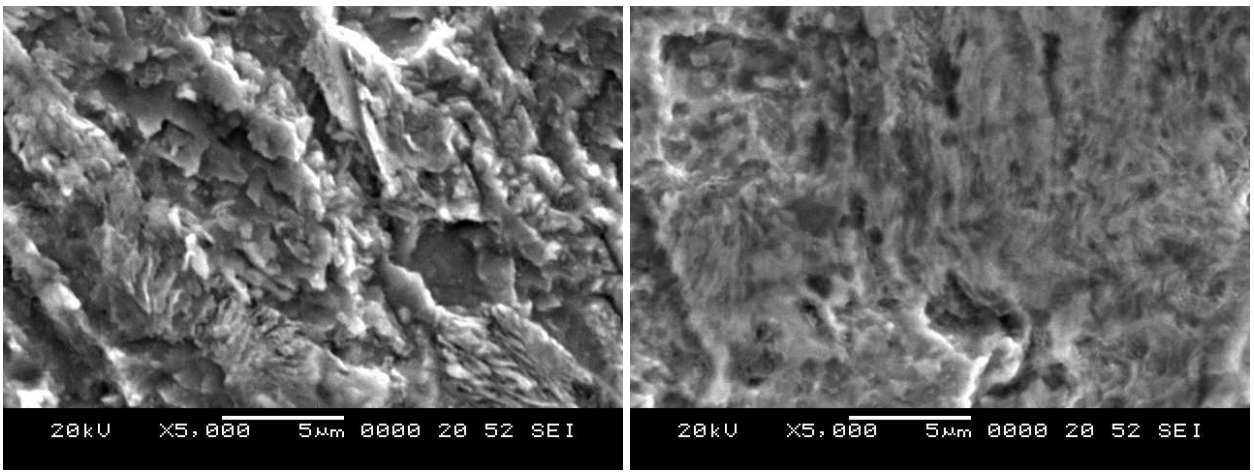

a **b**

Figure 12. Scanning electron microscopic images of mild steel immersed for 6 h in 1 M phosphoric acid (a) without and (b) with 800 ppm inhibitor

Based on the above-mentioned discussions a mechanism for the corrosion inhibition mechanism can be proposed. The plant extract molecules are believed to be present initially in the phosphoric acid solution. The dissolution of mild steel during the initial stages causes the formation of Fe^{2+}. The plant extract reacts with the Fe^{2+} ions and forms organo-metal complex (Fe-E) which forms a

layer on the metal surface. With increase in inhibitor concentration the surface coverage of the adsorbed layer increases [33].

$Fe^{2+} + E \rightarrow [Fe\text{-}E]$

This adsorbed layer again reacts with phosphate ions to form insoluble $FeHPO_4/FeH_2PO_4$ layer. Thus, the Fe-E complex acts as catalyst for the formation of iron phosphate complex [33]. Beyond certain inhibitor concentration the surface coverage of iron phosphate increases which results in decreased formation of Fe-E complex resulting in slight drop in efficiency [33].

4. CONCLUSIONS

- The alcoholic extract of *Pisidium guajava* (Guava) leaves was found to act as a good corrosion inhibitor for mild steel in 1 M phosphoric acid medium. A maximum inhibition efficiency of 89% was obtained for an inhibitor concentration of 800 ppm in the weight loss studies for 1 h immersion time.
- A drop in the inhibition efficiency with increasing temperature and an increase in apparent activation energy to 75 kJ mol^{-1} from 37.5 kJ mol^{-1} with the addition of 800 ppm inhibitor to 1 M phosphoric acid solution show that the corrosion reaction energy barrier is increased with the addition of inhibitor and the activation energy is in the range of comprehensive adsorption.
- Analysis of the system using Langmuir and Temkin adsorption isotherms yielded ΔG°_{ads} values ranging from -28 kJ mol^{-1} to -41 kJ mol^{-1} and heat of adsorption value of -61.2 kJ mol^{-1} which also shows that the adsorption is an intermediate type, which is a combination of physical and chemical adsorption.

ACKNOWLEDGEMENTS
The authors are grateful to Prof. S. Ramanathan, IIT-Madras for granting permission to conduct electrochemical experiments.

References

1. L.Y.S. Helen, A.A. Rahim, B. Saad, M.I. Saleh, P.B. Raja, *Int. J. Electrochem. Sci.,* 9 (2014) 830.
2. A.S. Yaro, A.A. Khadom, K.R. Wael, *Alexandria. Eng. J.*, 52 (2012) 129.
3. R.O. Ramos, A. Battistin, R.S. Gonçalves, *J. Solid State Electrochem.*, 16 (2012) 747.
4. D.M.O. Sotelo, J.G.G. Rodriguez, M.A.N. Flores, M. Casales, L. Martinez, A.V. Martinez, *J. Solid State Electrochem.*, 15 (2011) 997.
5. M. Abdeli , N.P. Ahmadi, R.A. Khosroshahi, *J. Solid State Electrochem*., 15 (2011) 867.
6. S.K. Shukla, E.E. Ebenso, *Int. J. Electrochem. Sci*., 6 (2011).
7. M. Abdeli , N.P. Ahmadi , R.A. Khosroshahi, *J. Solid State Electrochem*., 14 (2010) 1317.
8. P.C. Okafor, C.B. Liu, X. Liu, Y.G. Zheng, F. Wang, C.Y. Liu, F. Wang, *J. Solid State Electrochem.*, 14 (2010) 1367.
9. I. Ahamad, R. Prasad, M.A. Quraishi, *J. Solid State Electrochem*., 14 (2010) 2095.
10. I. Ahamad, R. Prasad, M.A. Quraishi, *Corros. Sci*., 52 (2010) 933.
11. N.O. Eddy, E.E. Ebenso, U.J. Ibok, *J. Argent. Chem. Soc*., 97 (2009) 178.
12. F.S. De Souza, A. Spinelli, *Corros. Sci*., 51 (2009) 642.
13. K.F. Khaled, *J. Solid State Electrochem.*, 13 (2009) 1743.

14. H.A. Sorkhabi, M. Eshaghi, *J. Solid State Electrochem.*, 13 (2009) 1297.
15. K.F. Khaled, *Int. J. Electrochem. Sci*., 3 (2008) 462.
16. M. O¨zcan, R. Solmaz, G. Kardas, I. Dehri, *Colloids Surf. A.*, 325 (2008) 57.
17. P.B. Raja, Sethuraman, *Mater. Lett.*, 62 (2008) 113.
18. S.T. Arab, A.M. Al-Turkustani, *Portugaliae Electrochim. Acta*, 24 (2008) 53.
19. L. Wang, *Corros. Sci*., 48 (2006) 608.
20. E.A. Noor, *Corros. Sci*., 47 (2005) 33.
21. K.K. Anupama, J. Abraham, *Res. Chem. Intermed*., 39 (2013) 4067.
22. M. Behpour, S.M. Ghoreishi, M. Khayatkashani, N. Soltani, *Mater. Chem. Phys*., 131 (2012) 621.
23. S. Deng, X. Li, *Corros. Sci*., 55 (2012) 407.
24. M.H. Hussin, M.J. Kassim, N.N. Razali, N.H. Dahon, D. Nasshorudin, *Arabian J. Chem*., DOI: 10.1016/j.arabjc.2011.07.002 (2011).
25. T.H. Ibrahim, M.A. Zour, *Int. J. Electrochem. Sci*., 6 (2011) 6442.
26. M.H. Hussin, M.J. Kassim, *Mater. Chem. Phys*., 125 (2011) 461.
27. A. Singh, I. Ahamad, V.K. Singh, M.A. Quraishi, *J. Solid State Electrochem*., 15 (2011) 1087.
28. P.C. Okafor, E.E. Ebenso, U.J.Ekpe, *Int. J. Electrochem. Sci*., 5 (2010) 978.
29. M.A. Quraishi, A. Singh, V.K. Singh, D.K. Yadav, A.K. Singh, *Mater. Chem. Phys*., 122 (2010) 114.
30. A.K. Satapathy, G. Gunasekaran, S.C. Sahoo, K. Amit, P.V. Rodrigues, *Corros. Sci*., 51 (2009) 2848.
31. P.C. Okafor, M.E. Ikpi, I.E. Uwah, E.E. Ebenso, U.J. Ekpe, S.A. Umoren, *Corros. Sci*., 50 (2008) 2310.
32. E.E. Oguzie, *Corros. Sci*., 50 (2008) 2993.
33. G. Gunasekaran, L.R. Chauhan, *Electrochim. Acta*., 49 (2004) 4387.
34. M.S.S. Morad, A. El-Hagag, A. Hermas, M.A.S. Aal, *J. Chem. Technol. Biotechnol*., 77 (2002) 486.
35. A.K. Singh, M.A. Quraishi, *Corros. Sci*., 52 (2010) 152.
36. R. Solmaz, *Corros. Sci*., 79 (2014) 169.
37. M. Bouklah, B. Hammouti, M. Lagren'ee, F. Bentiss, *Corros. Sci*., 48 (2006) 2831.
38. K.M. Ismail, *Electrochim. Acta*, 52 (2007) 7811.
39. R. Solmaz, G. Kardas, B. Yazici, M. Erbil, *Colloids Surf. A*, 312 (2008) 7.
40. X. Li, G. Mu, *Appl. Surf. Sci*., 252 (2005) 1254.
41. R. Solmaz, *Corros. Sci*., 81 (2014) 4.
42. R. Solmaz, *Corros. Sci.*, 52 (2010) 3321.
43. R.P. Venkatesh, B. Jun Cho, S. Ramanathan, Jin-Goo Park, *J. Electrochem. Soc*., 159 (2012) C447.
44. A. Sadkowski, *Solid State Ionics*, 176 (2005) 1987.
45. R. Sabino, B.S. Azambuja, R.S. Gonçalves, *J. Solid State Electrochem.*, 14, (2010) 1255.
46. M. Tourabi, K. Nohair, M. Traisnel, C. Jama, F. Bentiss, *Corros. Sci*., 75 (2013) 123.
47. R.M. Silverstein, F.X. Webster, D.J. Kiemle, *Spectrometric Identification of Organic Compounds*, John Wiley and Sons, USA (2005) p. 101.